COMANCHE and COCHISE : two reciprocal atmospheric codes for hyperspectral remote sensing

Laurent Poutier*, Christophe Miesch, Xavier Lenot, Véronique Achard, Yannick Boucher

Office National d'Etudes et de Recherches Aérospatiales, Département d'Optique Théorique et Appliquée

1. INTRODUCTION

This paper describes two reciprocal codes developed for hyperspectral imagery in remote sensing. The first one is called COMANCHE and computes the incoming spectral radiance at the sensor level, for an instrument operating in the VIS - LWIR spectral range and observing a target over a background. COMANCHE uses an analytical formulation of the upwelling radiance at the sensor level in which the atmospheric parameters are independent of the ground parameters. The formulation includes the environmental effects due to scattering (trapping effects and diffuse transmission). The atmospheric parameters are extracted from Modtran4 computations and the environment functions are obtained using two Monte-Carlo codes. The second code is called COCHISE and retrieves the 2D ground spectral reflectance from a calibrated hyperspectral image. The actual version of COCHISE is limited to the reflective domain. It performs the inversion of the COMANCHE analytical formulation and includes a 2D estimation of the columnar water vapor amount directly from the radiance hypercube. The COMANCHE and COCHISE algorithms are presented and preliminary validation results based on comparisons with reference radiative transfer codes and an AVIRIS data set are given.

2. ANALYTICAL FORMULATION OF THE AT-SENSOR RADIANCE

This section presents the formulation that is used in COMANCHE and that addresses the following scenario: the scene consists of a circular uniform lambertian target of radius R_t, albedo ρ_t and temperature T_t, laying on a uniform lambertian background, infinite in size, of albedo ρ_b and temperature T_b. The spectral radiance is simulated for a target pixel, centered on the target and a background pixel, located at such a distance from the target that adjacency effects involving the target material can be neglected.

For the target pixel, the incoming radiance, $L_{tot}^{tp}(\lambda)$, can be written as the sum of three contributors:

$$L_{tot}^{tp}(\lambda) = L_{atm}(\lambda) + t_{dir}(\lambda) L_0^{tp}(\lambda) + t_{dif}(\lambda) L_0^{env}(\lambda) \tag{1}$$

The first contributor, $L_{atm}(\lambda)$, represents the atmospheric radiance, without any interaction with the ground. The second one represents the upwelling radiance directly transmitted from the ground, which is the product of the direct transmission from the target to the sensor, $t_{dir}(\lambda)$, and the upwelling radiance at the ground level leaving the target pixel, denoted $L_0^{tp}(\lambda)$. The third contributor describes the photons that have reached the ground and then have been scattered towards the sensor. This contributor is the product of the diffuse upwelling transmittance $t_{dif}(\lambda)$ and the upwelling radiance of the target environment at the ground level, $L_0^{env}(\lambda)$.

The radiance leaving the target pixel is the sum of reflective and emissive terms, as written below:

$$L_0^{tp}(\lambda) = \tilde{\rho}^{tp}(\lambda) \frac{E_{tot}^{tp}(\lambda)}{\pi} + \tilde{\varepsilon}^{tp}(\lambda) L_{BB}\left(\lambda, \tilde{T}^{tp}(\lambda)\right) \tag{2}$$

* ONERA Centre de Toulouse, 2 av. Edouard Belin, BP 4025, 31055 Toulouse Cedex 4, France

Phone : (33) 5 62 25 26 25 ; Fax : (33) 562 25 25 88 ; E-mail : Laurent.Poutier@onecert.fr ; Web : http://onera.fr/dota-en/

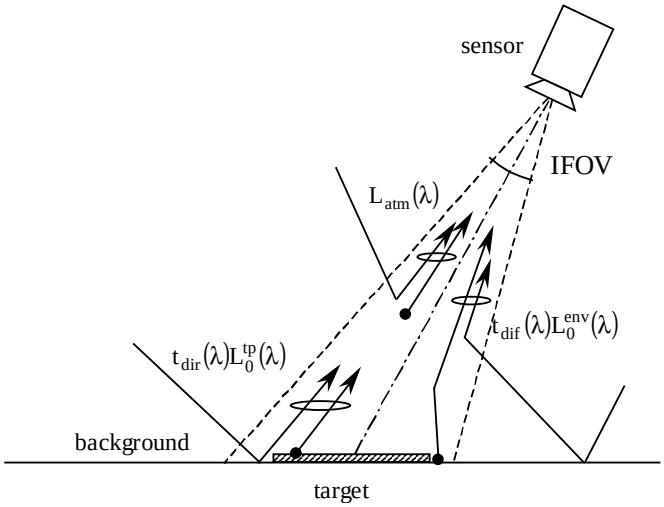

Figure 1. Illustration of the three contributors in the target pixel upwelling radiance.

In Eq. 2, $E_{tot}^{tp}(\lambda)$ represents the total irradiance incoming at the target pixel, $L_{BB}(\lambda,T)$ is the black body spectral radiance at temperature T, given by the Planck's law:

$$L_{BB}(\lambda,T)=\frac{A(\lambda)}{\exp[B(\lambda)/T]-1} \tag{3}$$

The terms $\tilde{\rho}^{tp}(\lambda)$, $\tilde{\varepsilon}^{tp}(\lambda)$ and $\tilde{T}^{tp}(\lambda)$ are respectively the albedo, the emissivity and the temperature averaged on the target pixel. Let α be simply the fraction of the target pixel corresponding to the target material. The three average thermo-optical characteristics of the target pixel are obtained as follow:

$$\tilde{\rho}^{tp}(\lambda)=\alpha.\rho_t(\lambda)+[1-\alpha].\rho_b(\lambda) \tag{4}$$

$$\tilde{\varepsilon}^{tp}(\lambda)=\alpha.\varepsilon_t(\lambda)+[1-\alpha].\varepsilon_b(\lambda) \tag{5}$$

$$\tilde{T}^{tp}(\lambda)=\frac{B(\lambda)}{\ln\left(\frac{A(\lambda).\tilde{\varepsilon}^{tp}(\lambda)}{\alpha.\varepsilon_t(\lambda)L_{BB}(\lambda,T_t)+[1-\alpha].\varepsilon_b(\lambda)L_{BB}(\lambda,T_b)}+1\right)} \tag{6}$$

The total downward irradiance can be written as:

$$E_{tot}^{tp}(\lambda)=\left[E_0(\lambda)+\pi\tilde{\varepsilon}_{dn}^{tp}(\lambda)L_{BB}\left(\lambda,\tilde{T}_{dn}^{tp}(\lambda)\right)S(\lambda)\right]\frac{1}{1-\tilde{\rho}_{dn}^{tp}(\lambda)S(\lambda)} \tag{7}$$

The first factor corresponds to the ground downward irradiance without ground reflection phenomena. It is the sum of $E_0(\lambda)$ which accounts for sun and atmospheric sources of irradiance, and of the surface emission scattered back to the ground through the atmospheric spherical albedo $S(\lambda)$. The second factor describes the trapping effects between the ground and the atmosphere.

The three quantities denoted as $\tilde{X}_{dn}^{tp}$ (albedo, emissivity and temperature) correspond to an averaging over the area participating in the trapping effect. Let the environment function $G_\lambda(r)$ describe the probability that the last reflection involved in the trapping effects comes from a distance r from the target center (there is no azimuthal dependence in the density function G_λ). The environment function describing the ground-atmosphere coupling should take into account the spatial distribution of the multiple rebounds that finally reach the target pixel. Meanwhile, as this function acts as a second order on the global irradiance (the spherical albedo being typically around or less than 10^{-1} in magnitude), it remains fully valid to describe it only by the last rebound, the multiple

trapping effects acting as a second order on the environment function, compared to the single rebounds. The average quantities can be obtained by the following formulas:

$$\tilde{\rho}_{dn}^{tp}(\lambda) = \alpha_{dn}(\lambda).\rho_t(\lambda) + [1-\alpha_{dn}(\lambda)].\rho_b(\lambda) \tag{8}$$

$$\tilde{\varepsilon}_{dn}^{tp}(\lambda) = \alpha_{dn}(\lambda).\varepsilon_t(\lambda) + [1-\alpha_{dn}(\lambda)].\varepsilon_b(\lambda) \tag{9}$$

$$\tilde{T}_{dn}^{tp}(\lambda) = \frac{B(\lambda)}{\ln\left(\frac{A(\lambda).\tilde{\varepsilon}_{dn}^{tp}(\lambda)}{\alpha_{dn}(\lambda).\varepsilon_t(\lambda)L_{BB}(\lambda,T_t) + [1-\alpha_{dn}(\lambda)].\varepsilon_b(\lambda)L_{BB}(\lambda,T_b)} + 1\right)} \tag{10}$$

where $\alpha_{dn}(\lambda)$ expresses the weight of the target material participating to the coupling effect:

$$\alpha_{dn}(\lambda) = 2\pi.\int_0^{R_t} G_\lambda(r).r.dr \tag{11}$$

The environment upwelling radiance $L_0^{env}(\lambda)$ is almost similar to the target pixel upwelling radiance. The main difference is that the averaging of the thermo-optical properties of the ground are governed by an environment function describing the spread out of the upwelling diffused radiance that reaches the sensor target pixel. In the same manner as in the trapping effect processes, let $F_\lambda(r,\theta)$ denote the 2D density function giving the probability that the upwelling diffuse paths come from the position (r,θ) expressed in polar coordinates relatively to the center of the target. The azimuthal dependence is observed for off-nadir viewing angles. In a similar way to Eq. 11, the weight of the target material involved in the diffuse radiance, $\alpha_{up}(\lambda)$, is derived by the following integration:

$$\alpha_{up}(\lambda) = \int_0^{2\pi}\int_0^{R_t} F_\lambda(r,\theta).r.dr.d\theta \tag{12}$$

The average thermo-optical properties implied in the environment upwelling radiance are given by:

$$\tilde{\rho}_{up}^{tp}(\lambda) = \alpha_{up}(\lambda).\rho_t(\lambda) + [1-\alpha_{up}(\lambda)].\rho_b(\lambda) \tag{13}$$

$$\tilde{\varepsilon}_{up}^{tp}(\lambda) = \alpha_{up}(\lambda).\varepsilon_t(\lambda) + [1-\alpha_{up}(\lambda)].\varepsilon_b(\lambda) \tag{14}$$

$$\tilde{T}_{up}^{tp}(\lambda) = \frac{B(\lambda)}{\ln\left(\frac{A(\lambda).\tilde{\varepsilon}_{up}^{tp}(\lambda)}{\alpha_{up}(\lambda).\varepsilon_t(\lambda)L_{BB}(\lambda,T_t) + [1-\alpha_{up}(\lambda)].\varepsilon_b(\lambda)L_{BB}(\lambda,T_b)} + 1\right)} \tag{15}$$

Finally, the environment upwelling radiance can be written as:

$$L_0^{env}(\lambda) = \tilde{\rho}_{up}^{tp}(\lambda)\frac{E_{tot}^{env}(\lambda)}{\pi} + \tilde{\varepsilon}_{up}^{tp}(\lambda)L_{BB}\left(\lambda,\tilde{T}_{up}^{tp}(\lambda)\right) \tag{16}$$

In the latter equation, the downward irradiance is denoted $E_{tot}^{env}(\lambda)$. In a strict formulation, the downwelling irradiance should include a position dependence, due to the coupling effects that, as mentioned before, involve an environment function related to the environment of the surface element where the irradiance is calculated. Considering that the joint effect of the ground-atmosphere coupling and the upwelling scattering are negligible, the downward irradiance is supposed to be uniform and equal to $E_{tot}^{tp}(\lambda)$ given by Eq.7.

Concerning the background pixel, the target interaction is neglected and the radiance is simply given by the precedent formulas where the coefficients α, $\alpha_{up}(\lambda)$ and $\alpha_{dn}(\lambda)$ are equal to zero.

3. DIRECT MODEL : COMANCHE IMPLEMENTATION

COMANCHE uses the precedent equations to simulate target/background at-sensor spectral radiances. These equations separate atmospheric radiative properties and ground characteristics. The atmospheric parameters are the upwelling atmospheric radiance without any interaction with the ground $L_{atm}(\lambda)$, the downwelling irradiance at ground level $E_0(\lambda)$, also with no interaction with the ground, the atmospheric spherical albedo $S(\lambda)$, the diffuse and direct upward transmittances, respectively $t_{dif}(\lambda)$ and $t_{dir}(\lambda)$, and the two environment functions $F_\lambda(r,\theta)$ and $G_\lambda(r)$.

The first five parameters are computed using the radiative transfer code Modtran4.1 (Anderson et al., 2000) in radiance mode, considering a uniform ground with four different boundary conditions: {ρ = 0, T = 0K} ; {ρ = 0.5, T = 0K} ; {ρ = 1, T = 0K} ; {ρ = 0, T = 300K}. Let $L_{tot}^{\rho,T}(\lambda)$ and $L_{ref}^{\rho,T}(\lambda)$ be respectively the total and reflected radiances associated to each simulation run. The direct transmittance is directly obtained as an output of the Modtran simulations. The atmospheric radiance is straightforward:

$$L_{atm}(\lambda) = L_{tot}^{0,0}(\lambda) \tag{17}$$

The spherical albedo is given by the relation:

$$S(\lambda) = \frac{L_{tot}^{1,0}(\lambda) + L_{tot}^{0,0}(\lambda) - 2.L_{tot}^{1/2,0}(\lambda)}{L_{tot}^{1,0}(\lambda) - L_{tot}^{1/2,0}(\lambda)} \tag{18}$$

The downward irradiance is given by:

$$E_0(\lambda) = \pi \frac{1 - S(\lambda)}{t_{dir}(\lambda)}.L_{ref}^{1,0}(\lambda) \tag{19}$$

The diffuse transmission is given by the following relation:

$$\begin{cases} t_{dif}(\lambda) = \dfrac{L_{tot}^{0,300}(\lambda) - L_{tot}^{0,0}(\lambda)}{L_{BB}(\lambda,300)} - t_{dir}(\lambda) & \text{if } \lambda \geq 3\mu m \\ t_{dif}(\lambda) = \left[L_{tot}^{1,0}(\lambda) - L_{tot}^{0,0}(\lambda)\right]\dfrac{1 - S(\lambda)}{E_0(\lambda)} - t_{dir}(\lambda) & \text{if } \lambda < 3\mu m \end{cases} \tag{20}$$

The environment functions $F_\lambda(r,\theta)$ and $G_\lambda(r)$ result from very complex and chaotic physical processes. Thus they are difficult to obtain directly from analytical expressions. Monte Carlo methods are well adapted to compute them in a robust way. Indeed, the Monte Carlo principle consists in modeling statistically the elementary phenomena to reproduce the global physical ones. In order to compute both environment functions, the method consists in simulating the paths of photons inside the atmosphere, considering a flat ground. Actually, the two algorithms developed here (one for each function) are derived from an existing radiative transfer code (Miesch et al, 1999). This radiative transfer code is able to simulate paths of photons inside the earth-atmosphere system and reproduce absorption, scattering and reflection phenomena. It considers a plane-parallel and horizontally invariant atmosphere divided into elementary homogeneous layers, and the extinction and scattering coefficients for both molecules and aerosols are computed at a specific monochromatic wavelength. The scene is represented by a digital elevation model associated to a bidirectional reflectance map. Each pixel of the ground model is assumed to be homogeneous.

To compute the environment function $F_\lambda(r,\theta)$, the existing algorithm is adapted so that the photons are launched from the sensor, in the viewing solid angle. The ground surface is digitized along the (r,θ) coordinates, in relation to the center of the observed ground pixel. Then, the photons that have been scattered by atmosphere and that have reached the ground surface are collected in each surface element. After having simulated enough paths to reach an acceptable convergence in the statistical process, the number of photons associated to a surface element divided by the total number of photons that have reached the ground is directly related to the values of the function $F_\lambda(r,\theta)$ over this surface element.

Concerning the environment function $G_\lambda(r)$, the photons have to be launched from a fixed point of the ground surface. As the ground is here supposed lambertian, the distribution of the emission direction is isotropic. Similarly to the previous computation, the ground surface is again digitized along the coordinate r, in relation to the initial emission point (there is here no dependence on the θ coordinate). The photons that are scattered back to the ground are collected in each annulus element. With an acceptable convergence, the values of the function $G_\lambda(r)$ are derived from the ratio of the photons collected in a given annulus and the photons received on the whole surface.

4. INVERSE MODEL : COCHISE IMPLEMENTATION

The global equation giving a pixel radiance in the reflective part of the spectrum can be rewritten as:

$$L_{tot}(x,y) = L_{atm} + t_{dir}.\left[\frac{E_0.\rho(x,y)}{\pi[1-\rho_G(x,y).S]}\right] + t_{dif}.\left[\frac{E_0.\rho_F(x,y)}{\pi[1-\rho_G(x,y).S]}\right] \quad (21)$$

This expression, limited to the VIS-NIR-SWIR, is reduced to the well-known 6S formulation (Vermote et al., 1997). The seven atmospheric parameters are obtained as in COMANCHE code except that the $L^{0,300}$ computation is no longer useful.

In Eq. 21, we have voluntarily omitted the wavelength dependence for clarity. Moreover, as this equation is to be inverted, the spatial dependence has been added through the (x,y) position of the pixel. The albedo $\rho(x,y)$ represents the averaged pixel albedo and the albedos $\rho_F(x,y)$ and $\rho_G(x,y)$ are the averaged values given by the convolutions with the environment functions introduced in the first section:

$$\rho_F(x,y) = \rho(x,y) \otimes F(x,y) \quad (22)$$

$$\rho_G(x,y) = \rho(x,y) \otimes G(x,y) \quad (23)$$

The inversion technique is iterative. In a first step, the adjacency effects are neglected and a first estimate of $\rho(x,y)$ is obtained by the following equation:

$$\hat{\rho}(x,y) = \frac{L_{tot}(x,y) - L_{atm}}{\frac{E_0}{\pi}.(t_{dir} + t_{dif}) + S\left(L_{tot}(x,y) - L_{atm}\right)} \quad (24)$$

Using Eq. 22 and Eq. 23 a first estimate of environment albedos $\hat{\rho}_F(x,y)$ and $\hat{\rho}_G(x,y)$ is calculated and reinjected in Eq. 21. A second estimate of $\rho(x,y)$ is then obtained by the straightforward inversion of Eq .21:

$$\hat{\rho}'(x,y) = \frac{\pi[1-\hat{\rho}_G(x,y).S]}{E_0.t_{dir}}.\left(L_{tot}(x,y) - L_{atm} - t_{dif}.\left[\frac{E_0.\hat{\rho}_F(x,y)}{\pi[1-\hat{\rho}_G(x,y).S]}\right]\right) \quad (25)$$

This last expression usually gives a satisfactory result. Meanwhile other iterations consisting in convoluting $\hat{\rho}'(x,y)$ with F and G and then reprocessing Eq. 25 could be performed to get a more accurate convergence.

As in COMANCHE, the seven atmospheric parameters, $t_{dir}(\lambda)$, $t_{dif}(\lambda)$, $E_0(\lambda)$, $L_{atm}(\lambda)$, $S(\lambda)$, $F_\lambda(x,y)$ and $G_\lambda(x,y)$ are first computed. The code also includes the inversion of the columnar water vapor amount on a pixel basis using spectral channels in an absorption band. As in FLAASH code (Adler-Golden et al., 1998), the retrieval uses a 2D Look-Up-Table depending on both reflectance and water vapor. The LUT is obtained in a preliminary training step: the at-sensor radiance in the appropriate channels is computed for a set of water vapor amounts and for different values of spectrally flat reflectances. A linear regression ratio (LIRR) and the mean radiance in the out-band channels (L_{REF}) are then computed and finally the LUT expresses the water vapor amount as a function of a regularly resampled grid {LIRR;L_{REF}}.

5. PRELIMINARY VALIDATION RESULTS

COMANCHE and COCHISE implement an analytical formulation relating ground properties and at-sensor radiances, where the atmospheric parameters are extracted from computations with a radiative transfer code (currently Modtran4.1) in four specific configurations (three for COCHISE). The first step of the validation consisted in verifying that the at-sensor radiance computed with COMANCHE was in good agreement with the one delivered by the radiative transfer code itself. Figure 2 gives the obtained differences between COMANCHE and Modtran4 for five different values of spectrally flat reflectance (0.0, 0.25, 0.5, 0.75 and 1.0), over the 0.4-13µm region. The comparison was performed for a homogeneous ground, a sensor located at 1.5 km above the ground and viewing at the nadir direction, a 30° sun zenithal angle, and a midlatitude summer model with 23 km visibility rural aerosols. The differences remain less than 0.4% and validate the at-sensor formulation for a homogeneous scene.

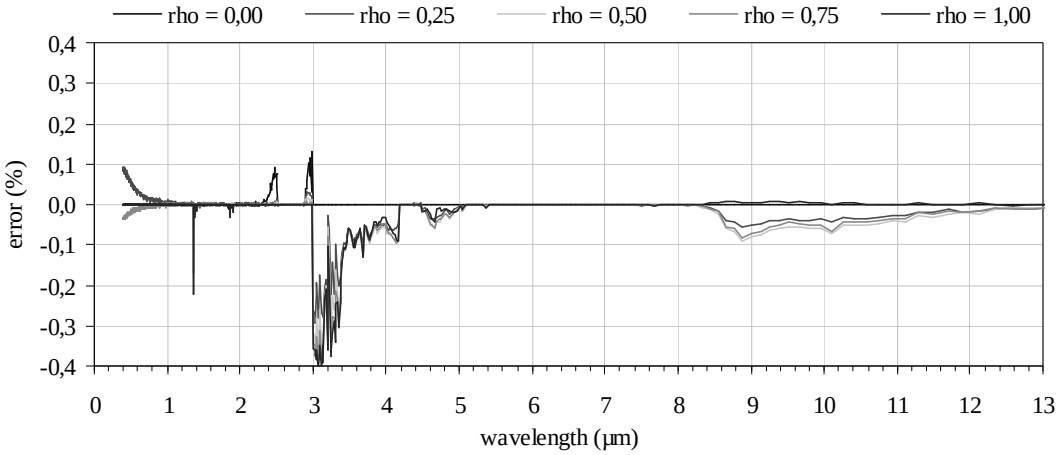

Figure 2. Comparisons between Modtran and COMANCHE at-sensor radiances for 5 reflectance values.

The second step consisted in verifying the reciprocity between COCHISE and COMANCHE in the COCHISE spectral domain (up to 2.5 µm). A uniform scene was simulated by duplicating COMANCHE outputs computed for the 224 AVIRIS channels in the environmental and geometric conditions of the previous validation step, for five reflectance values (0.1, 0.3, 0.5, 0.7, 0.9) and for four columnar water vapor amounts (1, 2, 3 and 4 g/cm^2). Figure 3 shows the water vapor then the reflectance sequentially retrieved by COCHISE. Residual errors for reflectance estimation in absorption bands are attributed to the spectral integration over the AVIRIS channels.

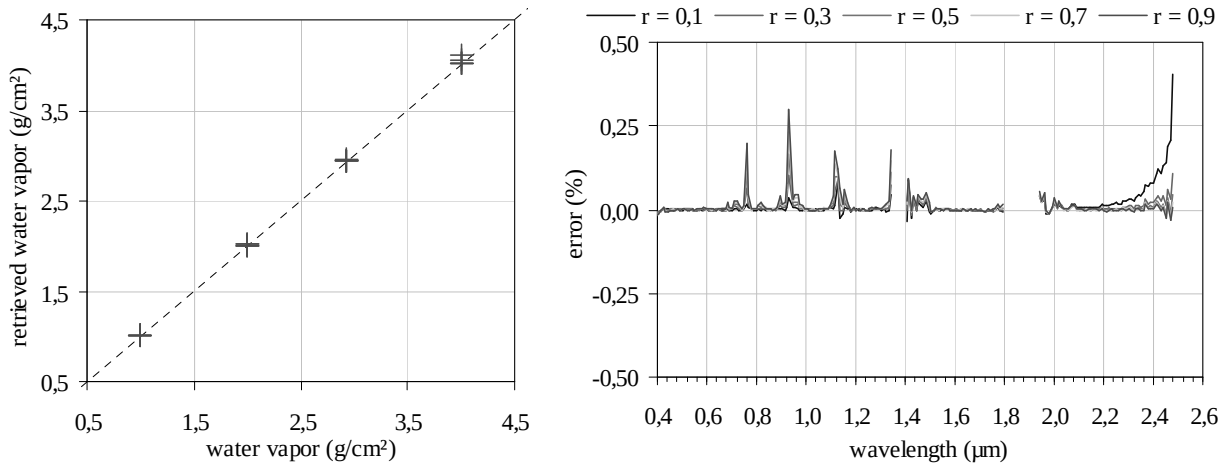

Figure 3. Evaluation of COCHISE on images simulated with COMANCHE for different water vapor and reflectance values. Retrieved water vapor (left), error on retrieved reflectance (right).

Further validations against a reference code have been carried out for heterogeneous scenes. They were based on AMARTIS that simulates at-sensor images in the VIS-NIR for heterogeneous 3D scenes including BRDF effects (Miesch et al., 2000). Figure 4 gives the comparison between AMARTIS and COMANCHE for a concrete target that fits exactly the target pixel, then occupies 1/9 of the same target pixel, the background being a standard vegetation. The simulation was done with the same conditions as the previous ones except the sensor altitude which was set to 3km. As AMARTIS is not dedicated to hyperspectral imagery, it was run for eight single wavelengths. The differences for the at-sensor radiance remain less than 5%. This amplitude is attributed to a difference in the spectral resolution of the two codes and a difference between the two top of atmosphere sun irradiance databases. Meanwhile, the observed differences keep the same amplitudes for the target and the background pixels. This validates the heterogeneous formulation applied to the target pixel which does not degrade the results compared to the standard homogeneous formulation for the background.

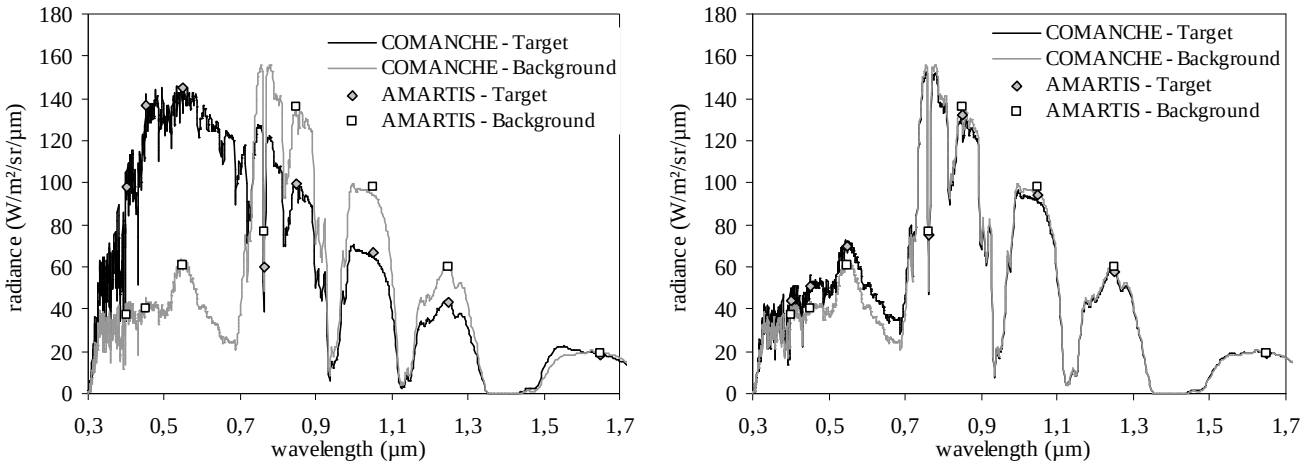

Figure 4. COMANCHE-AMARTIS comparisons for a heterogeneous scene. Target material coincident with target pixel (left) ; target material = 1/9 of target pixel pixel (right).

Concerning COCHISE, an image was simulated in the same conditions as before with AMARTIS, except that the geometry of the scene was an edge. Figure 5 shows the retrieved reflectance profile, normal to the edge. The adjacency effects are clearly apparent in the raw retrieval (after Eq. 23) and the convolution by the two environment kernels computed by the Monte-Carlo modules lead (after Eq. 25) to very satisfactory results, after only one iteration.

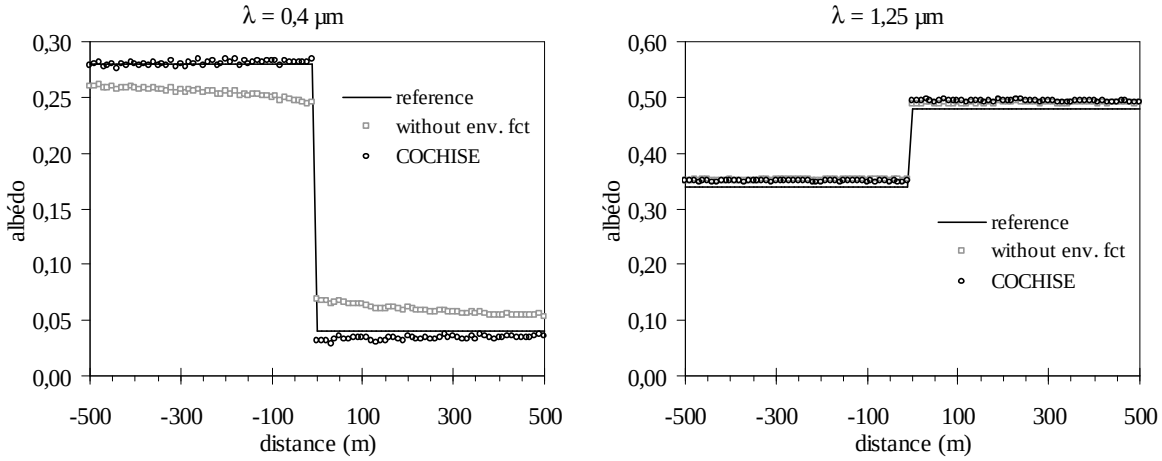

Figure 5. Retrieved reflectance with COCHISE, applied to an edge simulated by AMARTIS. Grey squares show the intermediate results without environment averaging.

Finally, COMANCHE and COCHISE have been applied to an AVIRIS data set composed of an AVIRIS radiance hypercube acquired over the Railroad Valley Playa on the 17 june 1998, a reflectance spectrum of the ground measured in laboratory and atmospheric characteristics including a radiosounding and optical depths measured at different wavelengths for constraining the aerosol behavior. The at-sensor radiance estimated by COMANCHE is shown on Figure 6, along with the radiance extracted from the pixel # (88, 463). The agreement is very good except for the first three channels and the difference is typically less than a few percents.

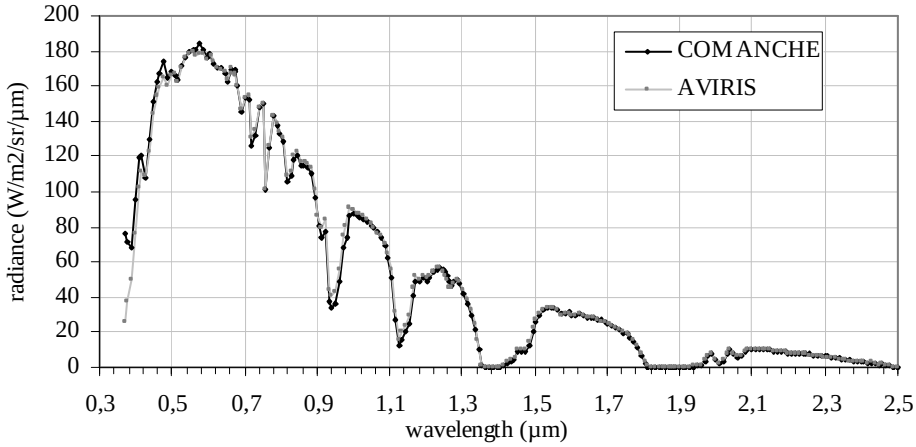

Figure 6. AVIRIS radiance and simulated radiance with COMANCHE.

The same data set is used for COCHISE. A first reflectance retrieval was computed using the water vapor included in the data set. Artifacts are observed in the H_2O absorption regions at 0.94 and 1.13µm. COCHISE was then rerun with a preliminary estimation of the water vapor content based on the 0.94µm absorption band. The restituted amount was 0.99g/cm² in the area of interest, with spatial variability of less than 5% within an extension of approx. 2x2 km. This value underestimates the original value (1.3 g/cm²) by nearly 25%. Meanwhile, the retrieved reflectance leads to a better fit in these two absorption bands. Figure 7 illustrates both reflectance spectra along with the ground truth. Correlatively to the radiance results (Figure 6) the retrieved reflectance is very close to the ground truth. The difference between the measured and estimated water vapor is currently under investigation.

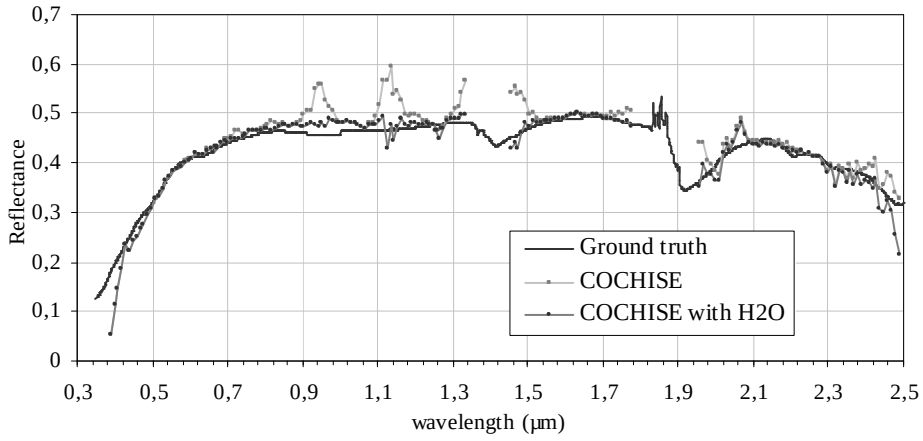

Figure 7. Reflectance retrieval with COCHISE, with and without water vapor correction, and AVIRIS ground truth.

6. CONCLUSION

A simple analytical formulation of the at-sensor radiance including reflective and emissive contributors is proposed for a target over a background. This formulation separates the atmospheric terms from the ground thermo-optical properties. This formulation has been implemented in a direct code, called COMANCHE, that is dedicated to hyperspectral contrasts evaluation in the VIS-LWIR domain. The atmospheric parameters are computed using the Modtran4.1 radiative transfer code and two Monte-Carlo modules estimate the spectral environment functions. The inversion of this formulation is straightforward in the reflective region and is implemented in COCHISE that also includes a water vapor retrieval module based on a 2D LUT. This code is devoted to large scale optical ground properties collection from hyperspectral remote sensing acquisitions.

Preliminary evaluations of these two reciprocal codes have been carried out: i) by confrontation with reference codes such as Modtran4 for homogeneous scenes and AMARTIS for heterogeneous scenes, ii) by comparison with an AVIRIS data set. The evaluation gave very satisfactory results in all of the studied cases. We then conclude that COMANCHE and COCHISE are validated in the VIS-NIR-SWIR region. Further comparisons will be completed on other experimental data sets including AVIRIS and HYMAP measurements. Moreover water vapor retrieval with COCHISE is still under investigation in order to compare results between the 0.94 and 1.13 µm.

Finally, the validation is still limited to homogeneous scenes in the infrared spectrum. An opportunity to overcome this limitation is to carry out comparisons with the MATISSE code developed at ONERA and that will be soon available (Simoneau et al., 2001).

7. ACKNOWLEDGEMENTS

The works associated with this paper are supported by the DGA, DSP/STTC/OP (Délegation Générale de l'Armement, Direction des Systèmes de forces et de la Prospective, Service Technique des Technologies Communes, Département Optronique). AVIRIS data on Railroad Valley Playa and ground-based measurements are courtesy of K. Thome, Optical Science Center, Remote Sensing Group, University of Arizona.

8. REFERENCES

Adler-Golden, S., A. Berk, L.S. Bernstein, S. Richtsmeier, P.K. Acharya, M.W. Matthew, G.P. Anderson, C.L. Allred, L.S. Jeong, J.H. Chetwynd, 1998, "FLAASH, a Modtran4 atmospheric correction package for hyperspectral data retrievals and simulations", 1998 AVIRIS Workshop Proceedings.

Anderson, G.P., A. Berk, P.K. Acharya, M.W. Matthew, L.S. Bernstein, J.H. Chetwynd, H. Dothe, S.M. Adler-Golden, A.J. Ratkowski, G.W. Felde, J.A. Gardner, M.L. Hoke, S.C. Richtsmeier, B. Pukall, J. Mello, L.S. Jeong, 2000, "MODTRAN4: Radiative transfer modeling for remote sensing", Algorithms for Multispectral, Hyperspectral, and Ultraspectral Imagery VI, Proceedings of SPIE, vol. 4049, pp. 176-183.

Miesch, C., X. Briottet, Y.H. Kerr, F. Cabot, 1999, "Monte Carlo approach for solving the radiative transfer equation over mountainous and heterogeneous areas", Applied Optics, Vol. 38, No. 36, pp. 7419-7430, 20 December 1999.

Miesch, C., X. Briottet, Y.H. Kerr, F. Cabot, 2000, "Radiative transfer solution for rugged and heterogeneous scene observations"; Applied Optics, Vol. 39, No.36, pp. 6830-6846, 20 December 2000.

Simoneau, P., R. Berton, K. Caillault, G. Durand, T. Huet, L. Labarre, C. Malherbe, C. Miesch, A. Roblin, B. Rosier, 2001, "MATISSE: Advanced earth modeling for imaging and scene simulation", Europto European Symposium on Remote Sensing, Toulouse, 17 21 September 2001.

Vermote, E., D. Tanré, J.L. Deuzé, M. Herman, J.J. Mocrette, 1997, "Second Simulation of the Satellite Signal in the Solar Spectrum (6S)", 6S User Guide Version 2.